Journal of Marine Research, 46, 429–455, 1988

A provisional diagenetic model for pH in anoxic porewaters: Application to the FOAM Site

by Bernard P. Boudreau[1,2] and Donald E. Canfield[3]

ABSTRACT

This paper presents a diffusion-advection-reaction model for the pH of anoxic porewaters in nonirrigated sediments. Because of the couplings demanded by the organic-matter decay reaction, various acid-base interconversions, dissolved-iron generation, and $CaCO_3$ and FeS precipitation, the model does not consider H^+ alone, but deals simultaneously with 17 dissolved species. The complex and largely unknown kinetics of some of the processes affecting these species have been approximated by simple *ad hoc* formulations. For this reason, the model must be considered provisional. We have also made extensive use of the local (partial) equilibrium assumption to circumvent the computational problems generated by rapid association/dissociation reactions.

The FOAM Site data are used as a vehicle to display the capabilities of this model. Assuming local equilibrium with FeS, the predicted pH profile is most sensitive to the reaction that liberates iron from the solid phase. The FOAM pH does not conform to a profile expected for any one iron-source mineral, but appears to reflect a composite source. Based on currently available data, this source might include magnetite and silicate minerals, but is unlikely to involve ferric oxides and hydroxides. The pH of FOAM porewaters is much less sensitive to the precipitation of FeS and $CaCO_3$ than would be suggested by past closed-system models.

The overall pH stability of anoxic porewaters is attributable to the fact that the dissolved products of organic-matter decomposition are added in such a way as to form a self-buffering mixture.

1. Introduction

Sulfidic porewaters (Berner, 1981) arise from the release of hydrogen sulfide, H_2S, during the microbial oxidation of organic matter by sulfate, SO_4^{2-}, reduction,

$$(CH_2O)(NH_3)_y(H_3PO_4)_z + \frac{1}{2}SO_4^{2-} \rightarrow HCO_3^- + \frac{1}{2}H_2S + yNH_3 + zH_3PO_4 \quad \text{(A)}$$

where the first reactant is average, metabolizable, organic matter and "y" and "z" are

1. Formerly: Department of Oceanography, University of British Columbia, Vancouver, British Columbia, Canada, V6T 1W5.

2. Present address: Department of Oceanography, Dalhousie University, Halifax, Nova Scotia, Canada, B3H 4J1.

3. Department of Geological Sciences, 1006 C. C. Little Building, University of Michigan, Ann Arbor, Michigan, 48109-1063, U.S.A.

stoichiometric coefficients. As written, two of the products of Reaction (A) are weak acids, H_2S and H_3PO_4, while a third is a weak base, NH_3. The final species, HCO_3^-, is amphoteric, capable of accepting or donating a proton.

The amount of each of these products added to porewaters by Reaction (A) can be considerable. The concentration of total dissolved sulfide, ΣH_2S, can attain 10 to 15 mM (e.g. Murray *et al.*, 1978). Total ammonia, ΣNH_3, may reach 3 mM in the zone of sulfate reduction (e.g. Goldhaber *et al.*, 1977), and the total dissolved carbon dioxide, ΣCO_2, may swell to 60 mM (e.g. Nissenbaum *et al.*, 1972).

At the same time, the pH of virtually all marine sulfidic porewaters is confined within fairly narrow limits, i.e. 7.0 to 8.2 (Ben-Yaakov, 1973). Considered in the light of the observed increases in protolytic species, this stability may appear surprising. Nevertheless, Thorstenson (1970), Nissenbaum *et al.*, (1972), Ben-Yaakov (1973) and Gardner (1973) have used closed-system thermodynamic and/or stoichiometric models to prove that the buffering capacity of anoxic sediments can account for this pH-stability.

Although these closed-system models are instructive, they cannot produce a profile of H^+ concentration or pH (i.e. concentration vs. depth in sediment). Nor can their results be accepted as quantitatively correct. A true diagenetic transport model that treats H^+ as a dependent variable is needed to accomplish these tasks.

The current lack of a diagenetic model for H^+ in anoxic porewaters can be attributed to its complexity. An appropriate model must not only treat the dissolved products of Reaction (A), but also their dissociation products, as well as OH^-, $B(OH)_3$ and $B(OH)_4^-$. Because iron sulfide and $CaCO_3$ precipitation reactions often occur coincidentally, the effects of these reactions on all dissolved species must be included; consequently, the model must be expanded to admit Fe^{2+} and Ca^{2+}. Therefore, the model must be more than a simple mathematical description of H^+ in porewaters; it must be an extensive accounting of the simultaneous behavior of all the dissolved species that are produced or affected by organic-matter decomposition in anoxic sediments.

Albeit a difficult undertaking, the formulation and solution of a diagenetic model for H^+ in anoxic porewaters is a highly desirable goal. It is required to obtain a quantitative answer to the old question of buffering capacity (Ben-Yaakov, 1973). Furthermore, H^+ is a minor species. Even if it is buffered, its concentration should reflect the balance of the chemical processes operating in sediments. The concurrent prediction of pH profiles with those of the other metabolic products would constitute a revealing test of our present paradigm for anoxic porewater chemistry. By considering concurrently all these dissolved species, we are forced to re-evaluate past modelling efforts where these same species were treated independently.

This paper advances a preliminary version of an H^+ model. We say preliminary because a set of restrictions and approximations have been adopted to overcome problems in three major areas. First, the model applies to nonirrigated sediment. The

complex reaction schemes in irrigated heterogeneous sediments are only now being unraveled (e.g. Aller and Rude, 1986). Secondly, the kinetics of Fe liberation and $CaCO_3$ precipitation in anoxic sediments have not been established experimentally. Finally, the effect of methanogenesis below the zone of sulfate reduction has not been included. We shall return to these points later. Beyond these imperfections, the model constitutes a reasonably good description of sulfidic interstitial waters.

Within this restricted framework, the model is applied to explain the porewater compositional data from the FOAM Site in Long Island Sound (see Goldhaber *et al.*, 1977; Aller 1980a, b; Krishnaswami *et al.*, 1984; Berner and Westrich, 1985, for details of this site). The FOAM data set is probably the most extensive and complete geochemical characterization of an anoxic sediment available in the literature. Yet, as we shall discover, the model tells us we may need even more information.

2. The model

The organic-matter decomposition Reaction (A) is accompanied by two other types of reactions. The first group encompasses reversible association/dissociation reactions for the weak acids/bases produced by decay (Table 1A).

The second type includes irreversible dissolution and precipitation reactions (Table 1B), such as the formation iron monosulfide (FeS) and $CaCO_3$. The precipitation of FeS demands a supply of Fe^{2+}. This iron must be provided *in situ* as porewaters at the top of the modelled sediment are essentially devoid of dissolved Fe^{2+} (Canfield, 1988). Part of the problems faced in applying our model is the identification of this source of iron. Hence, a variety of candidate minerals are considered below, and their Fe^{2+} liberation reactions are also listed in Table 1B.

The model assumes further that the sediments are in a steady state, that porosity is constant, and that complexation reactions can be ignored. This last assumption is probably incorrect for a few species (e.g. CO_3^{2-} and Ca^{2+}, Pytkowicz, 1983), but it is highly unlikely that the inclusion of complexation reactions (e.g. Lasaga, 1981a) will alter seriously our conclusions. Diffusive couplings demanded by neutral electronegativity requirements are also omitted (see Ben-Yaakov, 1972, 1981; Lasaga, 1979, 1981b; Katz and Ben-Yaakov, 1980; or Anderson, 1981) because these should constitute small corrections. Finally, we repeat that the model applies to sediment below the zone of bioturbation/irrigation.

Ion transport in porewaters is accomplished by molecular diffusion and advection due to burial. The net production and/or consumption of each dissolved species is balanced by the divergence of the flux caused by these transport processes. In our case, this generates a system of 17 coupled differential conservation equations (Table 2) for the 17 relevant species, i.e. H^+, OH^-, H_2S, HS^-, $CO_2(aq)$, HCO_3^-, CO_3^{2-}, Ca^{2+}, Fe^{2+}, NH_3, NH_4^+, H_3PO_4, $H_2PO_4^-$, HPO_4^{2-}, PO_4^{3-}, $B(OH)_3$ and $B(OH)_4^-$.

Note that in order to keep the equations within a reasonable size, the Lagrange (or

Table 1A. Reversible acid/base dissociation reactions included in our model of anoxic porewaters.

1) Carbonic Acid:

$$CO_2(aq) + H_2O \rightleftharpoons HCO_3^- + H^+ \quad (B)$$

$$HCO_3^- \rightleftharpoons CO_3^{2-} + H^+ \quad (C)$$

2) Hydrogen Sulfide:

$$H_2S \rightleftharpoons HS^- + H^+ \quad (D)$$

3) Ammonia:

$$NH_3 + H^+ \rightleftharpoons NH_4^+ \quad (E)$$

4) Water:

$$H_2O \rightleftharpoons OH^- + H^+ \quad (F)$$

5) Phosphoric Acid:

$$H_3PO_4 \rightleftharpoons H_2PO_4^- + H^+ \quad (G)$$

$$H_2PO_4^- \rightleftharpoons HPO_4^{2-} + H^+ \quad (H)$$

$$HPO_4^{2-} \rightleftharpoons PO_4^{3-} + H^+ \quad (I)$$

6) Boric Acid:

$$B(OH)_3 + H_2O \rightleftharpoons B(OH)_4^- + H^+ \quad (J)$$

Table 1B. Irreversible dissolution and precipitation reactions included in our model of anoxic porewaters.

1) Monosulfide:

$$Fe^{2+} + HS^- \rightarrow FeS(s) + H^+ \quad (K)$$

2) Carbonate:

$$Ca^{2+} + CO_3^{2-} \rightarrow CaCO_3(s) \quad (L)$$

3) Iron Liberation:

$$2\,Fe(OH)_3 + HS^- + 5\,H^+ \rightarrow 2\,Fe^{2+} + 6\,H_2O + S^0 \quad (M)$$

$$2\,FeOOH + HS^- + 5\,H^+ \rightarrow 2\,Fe^{2+} + 4\,H_2O + S^0 \quad (N)$$

$$2\,Fe_2O_3 + HS^- + 5\,H^+ \rightarrow 2\,Fe^{2+} + 3\,H_2O + S^0 \quad (O)$$

$$FeFe_2O_4 + HS^- + 7\,H^+ \rightarrow 3\,Fe^{2+} + 4\,H_2O + S^0 \quad (P)$$

$$KMgFe_2AlSi_3O_{10}(OH)_2 + 7\,H^+ + \tfrac{1}{2}\,H_2O \rightarrow K^+ + Mg^{2+} + 2\,Fe^{2+} + \tfrac{1}{2}\,Al_2Si_2O_5(OH)_4 + 2\,H_4SiO_4 \quad (Q)$$

$$Mg_2Fe_3Al_2Si_3O_{10}(OH)_8 + 10\,H^+ \rightarrow 2\,Mg^{2+} + 3\,Fe^{2+} + Al_2Si_2O_5(OH)_4 + H_4SiO_4 + 5\,H_2O \quad (R)$$

$$Fe^{2+}\text{-mineral} + \text{cation} \rightarrow \text{cation-mineral} + Fe^{2+} \quad (S)$$

Table 2. Diagenetic (conservation) equations governing the concentrations of the 17 dissolved species considered in our model of anoxic porewaters (Lagrange derivative notation).

$$D_H[H]'' - v[H]' - fR_{Fe} + R_{C1} + R_{C2} + R_S + R_W + R_{P1} + R_{P2} + R_{P3} + R_B - R_N + R_{FeS} = 0 \quad (1)$$

$$D_{OH}[OH]'' - v[OH]' + R_W = 0 \quad (2)$$

$$D_{H_2S}[H_2S]'' - v[H_2S]' + \tfrac{1}{2}\Sigma \alpha_i e^{-\beta_i x} - R_S = 0 \quad (3)$$

$$D_{HS}[HS]'' - v[HS]' - gR_{Fe} + R_S - R_{FeS} = 0 \quad (4)$$

$$D_{CO_2}[CO_2]'' - v[CO_2]' - R_{C1} = 0 \quad (5)$$

$$D_{HCO_3}[HCO_3]'' - v[HCO_3]' + R_{C1} - R_{C2} + \Sigma \alpha_i e^{-\beta_i x} = 0 \quad (6)$$

$$D_{CO_3}[CO_3]'' - v[CO_3]' + R_{C2} - R_{CaCO_3} = 0 \quad (7)$$

$$D_{Ca}[Ca]'' - v[Ca]' - R_{CaCO3} = 0 \quad (8)$$

$$D_{Fe}[Fe]'' - v[Fe]' + hR_{Fe} - R_{FeS} = 0 \quad (9)$$

$$D_{NH_3}[NH_3]'' - v[NH_3]' - R_N + y\Sigma \alpha_i e^{-\beta_i x} = 0 \quad (10)$$

$$D_{NH_4}[NH_4]'' - v(1 + K^N_{ads})[NH_4]' + R_N = 0 \quad (11)$$

$$D_{H_3PO_4}[H_3PO_4]'' - v[H_3PO_4]' - R_{P1} + z\Sigma \alpha_i e^{-\beta_i x} = 0 \quad (12)$$

$$D_{H_2PO_4}[H_2PO_4]'' - v(1 + K^P_{ads})[H_2PO_4]' + R_{P1} - R_{P2} = 0 \quad (13)$$

$$D_{HPO_4}[HPO_4]'' - v(1 + K^P_{ads})[HPO_4]' + R_{P2} - R_{P3} = 0 \quad (14)$$

$$D_{PO_4}[PO_4]'' - v(1 + K^P_{ads})[PO_4]' + R_{P3} = 0 \quad (15)$$

$$D_{B(OH)_3}[B(OH)_3]'' - v[B(OH)_3]' - R_B = 0 \quad (16)$$

$$D_{B(OH)_4}[B(OH)_4]'' - v[B(OH)_4]' + R_B = 0 \quad (17)$$

where:

D_j = tortuosity-corrected molecular diffusion-coefficient for species j ($cm^2 \cdot yr^{-1}$) ($D_j = D_j^0/\theta^2$)
D_j^0 = molecular diffusivity for species j ($cm^2 \cdot yr^{-1}$)
v = porewater burial velocity ($cm \cdot yr^{-1}$)
R = various reaction terms, see text ($mM \cdot yr^{-1}$)
K^N_{ads} = adsorption constant for NH_4^+ (dimensionless)
K^P_{ads} = adsorption constant for phosphate (dimensionless)
α_i, β_i = kinetic parameters for organic-matter decay by Reaction (A) ($mM \cdot yr^{-1}$ and cm^{-1}, respectively)
y, z = stoichiometric coefficients for Reaction (A)
f, g, h = stoichiometric coefficients for a iron source reaction chosen from Reactions (M) through (S)
θ = tortuosity (dimensionless)

prime) notation is used for spatial derivatives,

$$[C]' \equiv \frac{d[C]}{dx} \quad \text{and} \quad [C]'' \equiv \frac{d^2[C]}{dx^2}$$

where $[C] \equiv$ porewater concentration of species and $C \equiv H^+, OH^-$, etc.

The reaction terms R_{C1}, R_{C2}, R_S, R_N, R_W, R_{P1}, R_{P2}, R_{P3} and R_B represent the net rates (forward minus backward) of the reversible acid/base dissociation Reactions (B) through (J) in Table 1A, respectively. The explicit mathematical forms of these terms are probably complex nonlinear algebraic expressions involving many species (e.g. Johnson, 1982). Moreover, these reactions are recognized as rapid in natural waters (Horne, 1969). For example, Johnson (1982) has established that the characteristic time for the "slow" hydration step for CO_2, Reaction (B), is well under an hour. In this time, a typical ion diffuses no more than a millimeter.

An exact solution to a governing set of coupled nonlinear differential equations is improbable. In addition, the R-terms discussed above are likely to have large magnitudes compared to the other terms in each equation. This means that Eqs. (1) through (17) are numerically "stiff" and their solution is computationally difficult (Shampine and Gear, 1979).

Faced with similar difficulties in other chemical transport problems, past investigators have exploited the fact that association/dissociation Reactions (B) through (J) are fast and reversible so that thermodynamic equilibrium is maintained between the species involved in these reactions, even in the face of diffusion (e.g. Olander, 1960; Danckwerts, 1970; Otto and Quinn, 1971; DiToro, 1976; Chang and Rochelle, 1982; Rubin, 1983; Gallagher *et al.*, 1986; Boudreau, 1987). Accordingly, these R-terms are treated as unknown functions in Eqs. (1) through (17), and the resulting indeterminacy is resolved by assuming that the thermodynamic equilibrium relationships for Reactions (B) through (J) apply in the porewaters at each depth (Eqs. (18) through (26) in Table 3).

The rate of organic-matter oxidation, Reaction (A), is given by the sum of exponentials in Eqs. (3), (6), (10) and (12), i.e. $\Sigma\alpha_i e^{-\beta_i x}$. This exponential formulation is not mechanistic, but represents a convenient mathematical expression for regression analysis of reduction rate-data (Boudreau and Westrich, 1984).

Dissolved sulfide produced by Reaction (A) is subject to precipitation as solid sulfide minerals in the presence of available iron. The initial mineral formed is an amorphous iron monosulfide, FeS (Berner 1970, 1984; Goldhaber and Kaplan, 1974)

$$Fe^{2+} + HS^- \rightarrow FeS + H^+ \qquad (T)$$

Subsequently, this FeS may react with elemental sulfur, S^0, to generate pyrite, FeS_2

$$FeS + S^0 \rightarrow FeS_2 \qquad (U)$$

Indeed, virtually all the solid sulfide at the FOAM Site is present as pyrite (Goldhaber *et al.*, 1977; Westrich, 1983).

Table 3. Thermodynamic equilibrium relationships for Reactions (B) through (J), respectively.

$$K_{C1}\,[CO_2] = [HCO_3]\,[H] \tag{18}$$

$$K_{C2}\,[HCO_3] = [CO_3]\,[H] \tag{19}$$

$$K_S\,[H_2S] = [HS]\,[H] \tag{20}$$

$$K_N\,[NH_3]\,[H] = [NH_4] \tag{21}$$

$$K_W = [OH]\,[H] \tag{22}$$

$$K_{P1}\,[H_3PO_4] = [H_2PO_4]\,[H] \tag{23}$$

$$K_{P2}\,[H_2PO_4] = [HPO_4]\,[H] \tag{24}$$

$$K_{P3}\,[HPO_4] = [PO_4]\,[H] \tag{25}$$

$$K_B\,[B(OH)_3] = [B(OH)_4]\,[H] \tag{26}$$

Some aspects of the kinetics of Reactions (T) and (U) have been investigated by Pyzik and Summer (1981) and Rickard (1975), respectively. Their results indicate highly nonlinear rate expressions for these reactions. To a model already burdened by involved mathematics, this additional encumberment would severely compromise any currently available solution method. Fortunately, an alternative suggests itself. Berner (pers. commun.) notes that Reaction (T) is both fast and reversible. Consequently, we assume that Reaction (T) is locally in thermodynamic equilibrium, and that the pertinent dissolved species obey the relationship (Emerson *et al.*, 1983)

$$K_{FeS} = \frac{[H^+]}{[Fe^{2+}][HS^-]} \tag{27}$$

The rate term, R_{FeS}, in Eqs. (1), (4) and (9) is allowed to remain an unknown and Eq. (27) is employed to resolve the indeterminacy. This treatment is fully consistent with that developed by Berner (1980, p. 70–72) for solubility equilibrium between a salt and its constituent ions. Furthermore, the porewater data at the FOAM Site are not discordant with Eq. (27) (e.g. Aller, 1980b). We also assume for the purposes of the present calculations that precipitation of FeS is the only sink for dissolved sulfide. This has important consequences which we discuss later.

The R_{Fe}-term represents the rate of iron liberation by source-mineral dissolution or leaching. Many naturally occurring minerals can act as iron sources, including goethite (or lepidocrocite) (FeOOH), ferrihydrite (approx. $Fe(OH)_3$), hematite (Fe_2O_3), magnetite ($FeFe_2O_4$), biotite ($KMgFe_2AlSi_3O_{10}(OH)_2$), and chlorite ($Mg_2Fe_3Al_2Si_3O_{10}(OH)_8$). Amphiboles, pyroxenes, olivine, spinels and smectite cannot be considered important sources because of their scarcity or absence in FOAM sediments.

The overall liberation reaction for each of these minerals is shown in Table 1B. All involve some form of dissolution with the exception on Reaction (S). This last reaction

allows for the possibility that Fe^{2+} is leached-out without mineral dissolution (Drever, 1971; Heller-Kallai and Rozenson, 1978). With the exceptions of goethite (Rickard, 1974; Pyzik and Sommer, 1981) and magnetite (Canfield and Berner, 1987), the iron liberation reaction for these minerals has not been studied; nor has the actual source mineral(s) been identified for FOAM.

Faced with this ignorance, *ad hoc* measures are necessary. We assume that only one mineral acts as a source and that the rate of Fe^{2+} liberation is proportional to the rate of HS^- production by Reaction (A), $1/2\ \Sigma\alpha_i \exp(-\beta_i x)$, weighted by the stoichiometry of Reactions (M) through (S), i.e. constants f, g and h in Eqs. (1), (4) and (9).

Intuitively, R_{Fe} should be proportional to the HS^- and H^+ concentrations, not their production. Yet, the availability of dissolvable iron in the solid phase decreases with depth because reactive iron species are lost at the top of the sediment column, leaving more refractory material below. We believe that local availability controls the rate of iron release and this decreases with depth. To make it proportional to $\Sigma\alpha_i e^{-\beta_i x}$ is not unreasonable as a first guess.

Calcium-carbonate precipitation is inhibited in seawater (Berner, 1975; Berner *et al.*, 1978). At high enough levels of supersaturation, precipitation can occur (e.g. Sholkovitz, 1973). The kinetics of this process are not understood. Given this lack of a formal mathematical relationship, we adopt a simple exponential form:

$$R_{CaCO_3} = \kappa e^{-\epsilon x} \tag{28}$$

where κ and ϵ are adjusted to reproduce the Ca^{2+} data.

The total dissolved boron is treated as conservative whereas the two dissolved species of boron are allowed to interconvert. Boron may also be consumed by authigenic clay formation (Mackin, 1987). While this removal is assumed to be too small to affect our heavily buffered system, this supposition should be tested in future work if boron data are available.

Finally, we assume the concentration of all species is known at the base of the mixed zone,

$$[C] = C(0) \tag{29a}$$

and that all gradients disappear at infinity,

$$\left.\frac{d[C]}{dx}\right|_{x\to\infty} = 0 \tag{29b}$$

where C represents any and all dissolved species. A semianalytical iterative solution-method for the model is presented in the Appendix. As part of this method, the infinity condition, Eq. (29b), is applied at a great but finite depth, $x = L$.

3. FOAM Site characteristics

As remarked earlier, details of the location and geochemical characteristics of the FOAM Site are available in the papers by Goldhaber *et al.* (1977), Aller (1980a, b),

Krishnaswami *et al.* (1984), and Berner and Westrich (1985). Only a few germane properties are reviewed here.

The water is slightly more brackish than seawater (S‰ = 28.4, I = 0.57). This station is subject to seasonal fluctuations in temperature, with an annual mean of 12°C. This thermal modulation affects the rates of reaction and introduces chemical variations (Aller, 1980a, b). This transient is beyond the scope of the present model, and we restrict our attention to the annual mean behavior.

The sediment is primarily clay and silt with a small admixture of carbonate shell debris. The clay fraction is dominated by halloysite ($Al_2Si_2O_5(OH)_4$) and chlorite with lesser amounts of biotite, quartz and feldspar (M. Velbel cited in Westrich, 1983). With some equivocation, the burial velocity, v, is stated as 0.1 to 0.2 cm yr^{-1} (Krishnaswami *et al.*, 1984).

a. Parameter values. The model contains a large number of environmentally sensitive chemical parameters. The best estimates of these values for the FOAM Site are listed in Table 4, along with their sources. Our results are tolerant to moderately large errors in these values.

The diffusion coefficient for $B(OH)_3$ was not available at the time of our calculations. Since then, Mackin (1986a) has determined an experimental value of $D^0_{B(OH)_3} \simeq 353$ cm^2 yr^{-1}, which is within 10% of the estimated value in Table 4.

Finally, the rate of reaction (A) has been experimentally measured at the FOAM Site by Westrich (1983) and reported in Krishnaswami *et al.* (1984) and Berner and Westrich (1985) as

$$\sum_{i=1}^{2} \alpha_i e^{-\beta_i x} = 2\,(1.93\,e^{-0.055x} + 0.16\,e^{-0.006x}) \tag{30}$$

b. Porewater data. The composite porewater profiles for total ammonia (ΣNH_4), total phosphate (ΣPO_4), dissolved calcium (Ca^{2+}), total hydrogen sulfide (ΣH_2S), pH and total alkalinity (TAlk) are illustrated in Figures 1 through 6. Older data due to Goldhaber *et al.* (1977), Rosenfeld (1977), Berner *et al.* (1978), Martens *et al.* (1978) and Aller (1980a, b) are represented by the diamonds on these figures, while new data from Canfield (1988) correspond to the squares. The techniques of analysis are discussed in the references listed above and are not repeated here.

No dissolved iron data are shown. Recent analysis by Canfield (1988) reveals that the Fe^{2+} concentration is approximately 3 μM at the base of the irrigated layer, and falls precipitously below 1 μM (i.e. the detection limit) in just a few centimeters. The iron "data" can only be employed to place an upper limit on the model predictions. (The cause of the disagreement between these new data and the observations of Aller (1980b) is not known.)

The pH observations center on a value of 7.45 with noticeable scatter in the old data. Because of the log-scale, this implies large error in H^+ concentrations. This explains our reporting of pH rather than H^+.

Table 4. Values of the model parameters deemed appropriate for the FOAM Site.

		Source
1) Diffusion Coefficients: ($cm^2 \cdot yr^{-1}$)		
$D^0_{Ca} = 165$	$D^0_{CO_3} = 198$	Li and Gregory (1974)
$D^0_{Fe} = 149$	$D^0_{HCO_3} = 245$	corrected for salinity and
$D^0_{H_2PO_4} = 176$	$D^0_{HPO_4} = 153$	temperature, but not tor-
$D^0_{PO_4} = 127$	$D^0_H = 2023$	tuosity.
$D^0_{OH} = 1145$	$D^0_{NH_4} = 430$	
$D^0_{HS} = 376$		
$D^0_{H_3PO_4} = 273$	$D^0_{CO_2} = 400$	Based on the mutual coef-
$D^0_{NH_3} = 490$	$D^0_{H_2S} = 416$	ficients in Sherwood *et al.* (1975).
$D^0_{B(OH)_3} = 390$	$D^0_{B(OH)_4} = 340$	see text.
2) Activity Coefficients:		
$\gamma_H = 0.7$	$\gamma_{HS} = 0.67$	Millero (1983); Millero
$\gamma_{Fe} = 0.26$		and Schreiber (1982).
3) Apparent Equilibrium Constants: ($K = K'/\gamma_H$)		
$K'_{C1} = 7.58 \cdot 10^{-4}$ mM		Mehrbach *et al.* (1973).
$K'_{C2} = 4.13 \cdot 10^{-7}$ mM		ibid.
$K'_S = 1.33 \cdot 10^{-4}$ mM		Goldhaber and Kaplan (1975).
$K'_{P1} = 2.72 \cdot 10^{1}$ mM		Kester and Pytkowicz (1967).
$K'_{P2} = 0.66 \cdot 10^{-3}$ mM		ibid.
$K'_{P3} = 0.52 \cdot 10^{-6}$ mM		ibid.
$K'_B = 1.29 \cdot 10^{-6}$ mM		Lyman (1956).
$K'_N = 2.95 \cdot 10^{6}$ mM^{-1}		Morel (1983).
$K'_W = 1.29 \cdot 10^{-8}$ mM^2		Millero (1983).
4) Sulfide Solubility:		
$K_{FeS} = 0.237$ mM^{-1}		Emerson *et al.* (1983) but based on Berner (1967).
5) Adsorption Constants:		
$K^N_{ads} = 1.6$		Rosenfeld (1981).
$K^P_{ads} = 1.8$		Krom and Berner (1980).

In applying the model, we have favored the newer data from Canfield (1988). In particular, the old ΣH_2S data are much lower than the new set, and may reflect oxidation effects.

4. Model results

The curves in Figures 1 through 6 represent the model predictions for the FOAM porewaters. These are not statistically determined "best fits," but simple visual

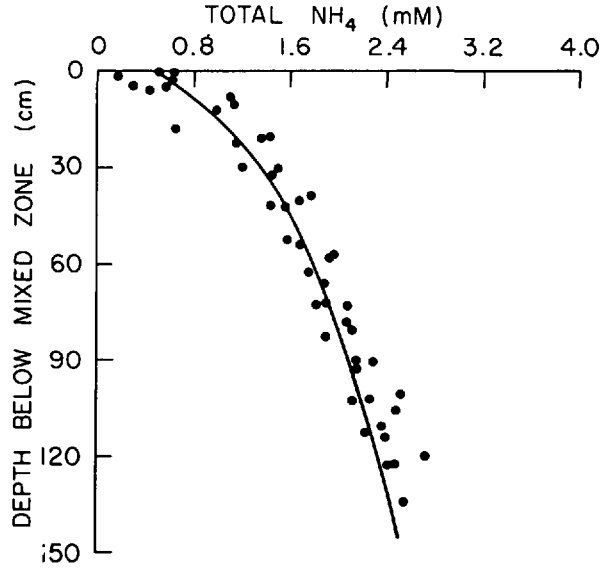

Figure 1. Total dissolved ammonia data (Goldhaber *et al.*, 1977; Rosenfeld, 1977; Aller, 1980a) and the model predicted profile for the FOAM Site. The N:C ratio of the organic matter is calculated to be 12.5/106.

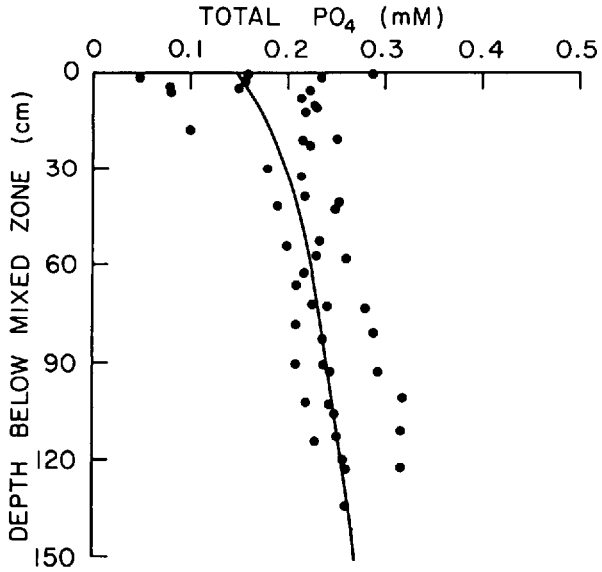

Figure 2. Total dissolved phosphate (Goldhaber *et al.*, 1977; Rosenfeld, 1977; Aller, 1980a) and the model predicted profile for the FOAM Site. The P:C ratio of the organic matter is calculated to be 0.3/106.

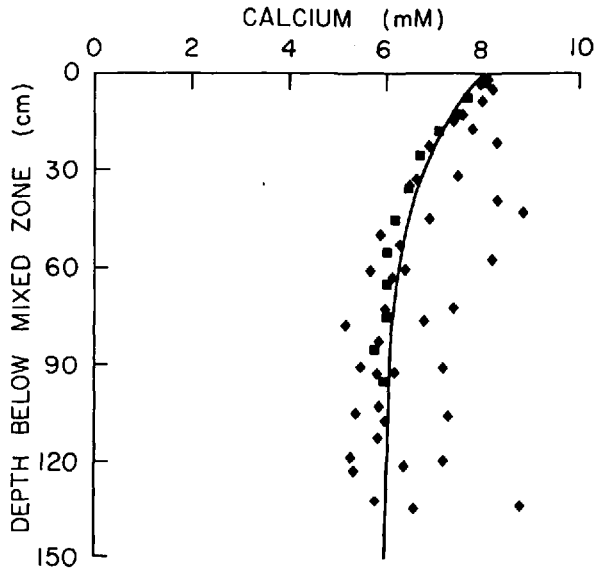

Figure 3. Dissolved calcium data (diamonds for Berner *et al.*, 1978; Aller, 1980a; squares for Canfield, 1988) and the model predicted profile for the FOAM Site.

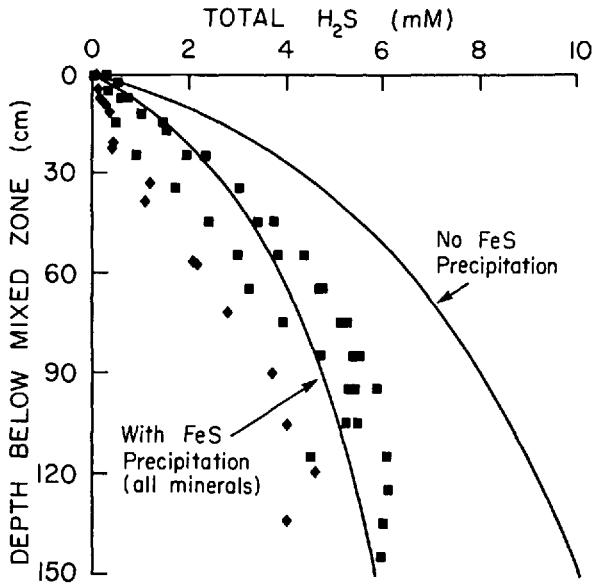

Figure 4. Total dissolved sulfide data (diamonds for Goldhaber *et al.*, 1977; Martens *et al.*, 1978; squares for Canfield, 1988) and model predicted profiles for the FOAM Site. The curve labelled "No FeS Precipitation" represents the potential ΣH_2S profile if the sulfide generated by sulfate reduction did not precipitate as FeS. The curve labelled "FeS Precipitation" is the best fit allowing FeS to form.

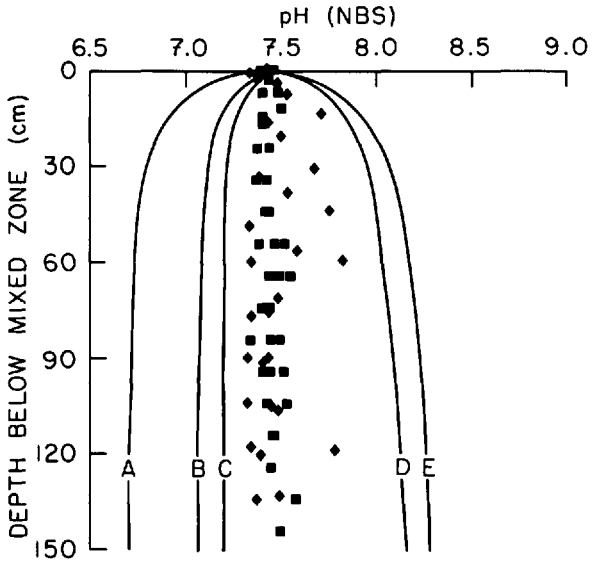

Figure 5. pH data (diamonds for Berner *et al.*, 1978; Martens *et al.*, 1978; Aller, 1980a; squares for Canfield, 1988) and the model predicted profiles for the FOAM Site for each of the iron-liberation reactions in Table 1B. Curve A is for exchange (Reaction S), Curve B for no FeS or $CaCO_3$ precipitation, Curve C for ferrihydrite, goethite, hematite and magnetite (Reactions M, N, O and P, respectively), Curve D for chlorite (Reaction R) and Curve E for biotite (Reaction Q).

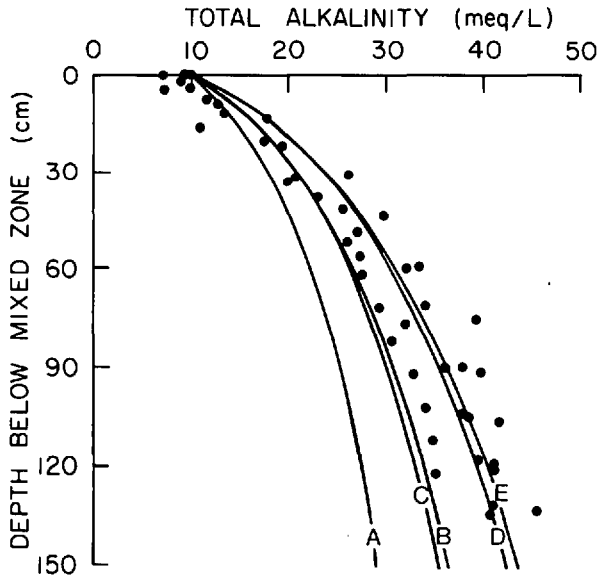

Figure 6. Total alkalinity data (Goldhaber *et al.*, 1977; Berner *et al.*, 1978; Martens *et al.*, 1978; Aller, 1980a) and the model predicted profiles for the FOAM Site for each of the iron-liberation reactions in Table 1B. Key in Figure 5.

estimates. A statistical treatment would demand an enormous effort that may not be successful and may not produce significantly better conformity to the data.

a. Ammonia and phosphate. The ΣNH_4 and ΣPO_4 predictions were obtained by assigning values of 12.5/106 and 0.3/106, respectively to the stoichiometric coefficients y and z for Reaction (A). Both values are lower than the C:N:P ratio given by Redfield *et al.* (1963) for average marine plankton, i.e. 106:16:1, and that measured for plankton in Long Island Sound, i.e. 106: 15.1:0.93 (Krom and Berner, 1981). This depletion in nitrogen and phosphorus is thought by Berner (1977) and Krom and Berner (1981) to occur in the water column and/or in the mixed layer.

At the same time, the N:C ratio utilized in the present model is higher than that calculated by Krom and Berner (1981) for the FOAM Site, but in agreement with the earlier calculations of Berner (1977). Conversely, the P:C ratio agrees with that of Krom and Berner (1981), while being distinctly smaller than that of Berner (1977). Because each study considered a different set of data, perfect agreement should not be expected. All studies agree on the magnitude of the depletion. In the current model, a N:C ratio as low as 10.7/106 (Krom and Berner, 1981) or a P:C ratio as high as 0.75/106 would produce unacceptable curves.

b. Calcium. As noted earlier, the Ca^{2+} profile is produced by adjusting the parameters in Eq. (28). The optimal values of the parameters are approximately $\kappa = 0.2$ mM yr^{-1} and $\epsilon = 0.03$ cm^{-1}.

c. Dissolved sulfide. Figure 4 displays two model predicted curves. One is the ΣH_2S-profile that would be expected without any FeS precipitation and the other is the best fit with sulfide formation. Each iron-source mineral was made to reproduce this latter curve.

The curve without FeS precipitation is included as a check for the validity of the model. In the complex model given in Table 2, there is no simple stoichiometric relationship between the total change of ΣH_2S with depth without FeS formation, $\Delta\Sigma H_2S$, and the decrease in dissolved sulfate, ΔSO_4. However, if porewater advection is ignored then, as an order of magnitude estimate,

$$\Delta SO_4 \simeq \frac{\overline{D}^0_{\Sigma H_2S}}{D^0_{SO_4}} \Delta\Sigma H_2S \text{ (no FeS ppt)} \tag{31}$$

where $\overline{D}^0_{\Sigma H_2S}$ is the average free-diffusion coefficient for the dissolved sulfide species weighted by their relative abundances, i.e. $\overline{D}^0_{\Sigma H_2S} \simeq 400$ cm^2 yr^{-1}. The free-diffusion coefficient for sulfate, $D^0_{SO_4}$, is approximately equal to 220 cm^2 yr^{-1} (Li and Gregory, 1974), so that $\overline{D}^0_{\Sigma H_2S}/D^0_{SO_4} \simeq 1.8$.

From Goldhaber *et al.* (1977), $\Delta SO_4 \simeq 20$ mM. Eq. (31) predicts a $\Delta\Sigma H_2S$ of 11 mM, while our model predicts that, in the absence of FeS precipitation, ΣH_2S

increases by about 10 mM. The reasonably good agreement between the present model and our intuitive argument based on chemistry and observation would be even better if we could account for the effects of advection in Eq. (31).

The model fit to the ΣH_2S data (the other curve in Fig. 4) is produced by assuming that FeS precipitation is the only sink for dissolved sulfide. This would require the liberation of 0.3 to 0.7 wt. % Fe from the solid phase between the base of the mixed layer and about 1.5 m depth. As we shall discuss later, not all the ΣH_2S may be removed by FeS precipitation.

d. pH. The only free parameters available in fitting the pH profile are the stoichiometric coefficients *f*, *g* and *h* which characterize the iron-liberation reaction. These are not independent parameters, and once an iron-source mineral is chosen, they become fixed. The predicted pH profile for each reaction in Table 1B is shown in Figure 5.

e. Alkalinity. There are no free-parameters available to alter the TAlk-curves once the other profiles have been adjusted. The model results are illustrated in Figure 6. The sequence of model curves is nearly identical to that of pH. This reflects the effect of pH on the extent of dissociation of weak acids and bases in the porewaters.

The change in TAlk, ΔTAlk, is somewhere between 30 and 40 mM, and is mostly due to an increase in HCO_3^-. Based on intuitive arguments, the change in alkalinity should be related to the change in total dissolved sulfide. Ignoring advection, this balance in the absence of FeS precipitation is approximately,

$$\Delta \mathrm{TAlk} \simeq 2 \frac{\overline{D}^0_{\Sigma H_2S}}{\overline{D}^0_{\mathrm{TAlk}}} \Delta \Sigma H_2S \text{ (no FeS ppt)} \tag{32}$$

where $\overline{D}^0_{\mathrm{TAlk}}$ is the abundance-weighted diffusion coefficient of the species in TAlk, i.e. $\overline{D}^0_{\mathrm{TAlk}} \simeq 225$ cm^2 yr^{-1}. With ΔH_2S of 10 mM, Eq. (32) predicts a ΔTAlk of 36 mM, which is within the observed range. These checks assure us that the model of Table 2 provides a reasonable description of reality.

In addition to the data and predictions of Figures 1 through 6, we also calculated the saturation state of the porewaters with respect to calcite. Below the mixed layer, the porewaters remain supersaturated at all depths except if the exchange reaction (Reaction S) is the dominant source of iron. Contrast this to the undersaturation in the mixed layer calculated by Aller (1982).

5. Discussion

a. pH results. If our hope had been to produce a simple explanation for the pH in the FOAM porewaters, then Figure 5 has surely disillusioned us. Under the chosen model assumptions, the results in this figure indicate that the pH is strongly dependent on the

mode on iron liberation. Iron release solely without mineral destruction (e.g. by exchange) leads to pH-values as low as 6.5. Dissolution and reduction of iron oxides and oxyhydroxides generates higher pH (i.e. ~ 7.25), but still lower than the data. The silicate iron-sources produce pH profiles that are far greater than the observed.

Evidence on iron availability collected by Canfield (1988) argues that ferric oxides and oxyhydroxides are not present at FOAM in measurable quantities below the mixed layer depth. Reactive magnetite is restricted to the upper 30 cm (Canfield and Berner, 1987). In addition, Canfield (1988) has observed the conversion of biotite to pyrite by SEM/EDS examination.

If the basic assumptions of our model are correct, then no single mineral dominates iron liberation at the FOAM Site. Instead, the iron needed for sulfide formation is probably supplied by a sequence of minerals that act as sources on overlapping depth ranges. In particular, our prejudices favor magnetite dissolution, silicate "weathering" and some form of exchange. Consequently, the pH profile reflects the integrated effects of a complex of iron source-reactions. The model can be modified to include a depth-dependent distribution of more than one iron mineral. Due to the speculative nature of our proposed iron sources, we have chosen not to pursue this matter without more data.

Past closed-system models by Ben-Yaakov (1973) and Gardner (1973) have suggested prominent roles for FeS and $CaCO_3$ precipitation in determining porewater pH. Specifically, Ben-Yaakov's (1973) closed-stoichiometric model predicts that while $CaCO_3$ precipitation acts to lower pH, sulfide precipitation will increase the pH.

The influences of these two processes in our open-system model are explored partially in Figure 7. Curve 2 in this diagram is produced with no FeS or $CaCO_3$ precipitation. If FeS is allowed to precipitate with the ambient dissolved iron but without concurrent iron liberation or $CaCO_3$ formation, then the profile is shifted about 0.01 pH units to the left of Curve 2 (i.e. this is indistinguishable from Curve 2 with the current scale). The superposition of $CaCO_3$ precipitation required to explain the FOAM Ca^{2+} profile moves the profile ~0.1 pH unit lower to Curve 1. Therefore, the mere introduction of these precipitation reactions does not appear to have a pronounced effect on the pH profile (although the effect on the H^+ concentration is large in this pH range).

The addition of magnetite dissolution as an iron liberation reaction moves the profile to higher pH, i.e. ~0.125 pH units with accompanying $CaCO_3$ precipitation (Fig. 7, Curve 3) and ~0.25 pH units without (Fig. 7, Curve 4). The effect of the iron-liberation reaction is greater than FeS precipitation in determining pH (at least in this pH range). The net effect of producing solid sulfide from the ΣH_2S generated by sulfate reduction and the iron liberated subsequently is to raise not lower the pH (unless Fe^{2+} originates from the exchange reaction).

Both journal reviewers of this paper faulted our model for the exclusion of H^+-silicate reactions that are independent of H_2S. The case for silicate pH-buffering

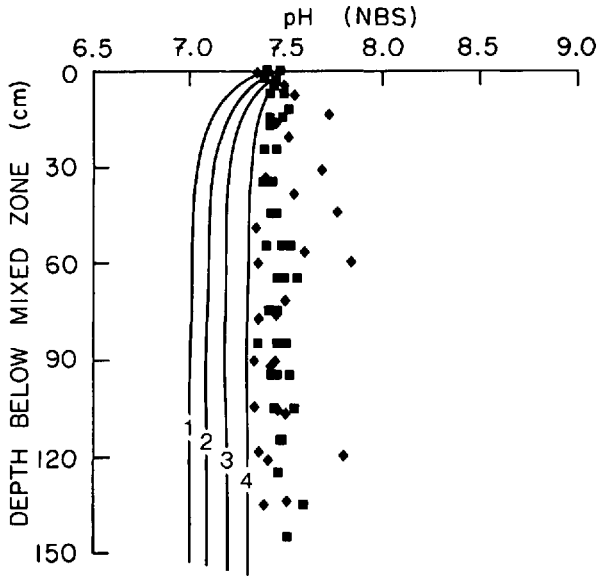

Figure 7. Illustration of the effect of the presence and absence of $CaCO_3$ and FeS precipitation on the pH at the Foam Site. Curve 1 is generated with no Fe^{2+} liberation, but with both $CaCO_3$ and FeS formation. Curve 2 has neither FeS nor $CaCO_3$ precipitation. Curve 3 results from Fe^{2+} liberation from magnetite and concurrent precipitation of both FeS and $CaCO_3$. Curve 4 is the same as Curve 3, but without $CaCO_3$ formation.

has been strongly advanced by Mackin and Aller (1984) and Mackin (1986b) in the form of equilibrium silicate dissolution/precipitation. More recently, Mackin and Swider (1987) have further proposed that equilibrium adsorption of H^+ on exposed Al-octahedra of silicate minerals should also provided buffering. In addition, there remains the possibility of "reverse weathering" reactions (Mackenzie and Garrels, 1966), although we feel this is unlikely in FOAM sediments.

We agree that the disregard of H^+-silicate reactions constitutes a glaring omission and reflects our ignorance of the appropriate choice of reaction(s) at FOAM, and an absence of the necessary porewater and solid phase data (e.g. dissolved Al). The stability of the final pH of anoxic porewaters (7–7.5) argues for additional buffering capacity beyond that present in our model (Fig. 5); perhaps this may be found in silicate reactions.

b. Sulfide mass balance. Let us now return to the assumption that the deficit between the actual ΣH_2S profile and that predicted without any precipitation is due entirely to the formation of FeS. This assumption leads to a mass balance problem. Iron-liberation Reactions (M), (N), (O), and (P) supply at most only half the elemental sulfur needed to convert the FeS to pyrite by Reaction (U), while Reactions (Q), (R)

and (S) generate no elemental sulfur at all. At the same time, the conversion of FeS to FeS_2 is essentially complete at FOAM (Goldhaber *et al.*, 1977; Westrich, 1983).

This strain on the S^0 mass balance can be resolved in two ways. First, we can assume that the measured rate of sulfate reduction is solely a measure of Reaction (A) and that the H_2S production is correct as modelled. Then a sink for ΣH_2S other than FeS must be identified. To this effect, Boulegue *et al.* (1982), Rudd *et al.* (1986) and Francois (1987) show that various amounts of hydrogen sulfide can be removed by reaction with organic compounds.

At the same time, S^0 might be supplied by diffusion from the mixed zone where sulfate reduction is more intense and oxidizing species more prevalent. We are unsure of the role played by these processes at the FOAM Site. However, there is no evidence to support the contention that O_2 can be supplied by irrigation into the historic layer to react with ΣH_2S and produce the required S^0. Unlike the NWC and DEEP Sites in Long Island Sound, FOAM sediments do not appear to be penetrated by actively irrigated burrows below 15 cm (Krishnaswami *et al.*, 1984).

Alternatively, it is tempting to assume that part of the SO_4^{2-} is reduced to S^0 rather than H_2S. Attractive as this possibility might be in solving our mass balance enigma, such a reaction has never been shown to occur naturally (B. B. Jorgensen, pers. commun.; M. Goldhaber, pers. commun.).

Another enticing possibility is the reduction of sulfate by an agent other than organic matter, for example by reaction with either HS^- or CH_4 to produce S^0. Such reactions would appear to require biological mediation. However, because the conversion of FeS to FeS_2 is essentially complete above the depth where SO_4^{2-} and CH_4 coexist, this latter process is of no real importance at FOAM, if it occurs at all.

Finally, inaccuracies may result from our neglect of methanogenesis and the assumption that solid organic matter is the only substrate for metabolism. Methanogenesis often occurs below the zone of sulfate reduction by an overall reaction.

$$(CH_2O)_{106}(NH_3)_{16}(H_3PO_4) \rightarrow 53\ CO_2 + 53\ CH_4 + 16\ NH_3 + H_3PO_4 \qquad (V)$$

The products and stoichiometry of Reaction (V) are appreciably different than those of Reaction (A). Although the H_2S released by Reaction (A) appears to negate the potential pH rise due to ammonia production (Berner, 1969), it is not obvious that the CO_2 generated by Reaction (V) can accomplish the same task. However, the data of Berner *et al.* (1970) do not indicate an unusual pH rise in Somes Sound sediments where ΣNH_4 reaches 11.4 mM.

Reebergh (1976, 1980), Murray *et al.* (1978), Devol *et al.* (1984), Martens and Klump (1984) and Iversen and Jorgensen (1985) all advance proof that the methane from Reaction (V) may act as a metabolic substrate via a reaction of the form

$$CH_4 + SO_4^{2-} \rightarrow HS^- + HCO_3^- + H_2O \qquad (W)$$

The second exponential in the FOAM sulfate-reduction rate-expression, Eq. (29), may be due to this reaction.

Reaction (W) involves no new products when compared to Reaction (A), but the stoichiometry is different and NH_4 is not generated. This is unlikely to cause a large change in the predicted pH, yet it does suggest another area for future investigation.

6. Concluding remarks

The conclusions listed below must be considered tentative because they are based on a particular form of the pH model. Most importantly, this model ignores direct H^+-silicate reactions and assumes exclusive removal of ΣH_2S by FeS formation.

First, we must agree with Ben-Yaakov (1973, p. 89–90) that the pH buffering of anoxic porewaters with respect to the protolytic products of organic-matter decay "results from the fact that the various components enter the system in a constant proportion, when the initial concentration of weak acids and bases is small in comparison to" that added by decomposition.

Secondly, those factors which adjust pH appear to operate near the top of the historical layer. The result is that the pH profiles are essentially vertical below ten to twenty centimeters depth although organic decay continues at measurable rates.

Thirdly, the reactions responsible for iron-liberation have the greatest potential influence on the pH-value reached at depth in the porewaters. However, no particular iron mineral can be identified as the pre-eminent source below the mixed layer at FOAM. The pH profile must be a composite caused by a variety of minerals which excludes ferric oxides and oxyhydroxides. The study of pH in sulfidic sediments cannot be separated from an understanding of the iron geochemistry.

Finally, closed system models predict quantitatively significant alterations in pH with variations in the amount of $CaCO_3$ and FeS precipitated. The present open-system diagenetic model indicates much greater stability for FOAM type sediments with respect to these two processes.

The model presented in this paper is preliminary and needs to be improved in a number of areas. Appropriate iron liberation and $CaCO_3$ precipitation kinetics must be established and incorporated into the model. Methanogenesis and its consequences should be addressed. The model must also be extended to account for the many pH-modifying processes in the irrigated zone.

The value of a pH model does not lie solely in its ability to predict H^+ profiles. A pH model is a comprehensive mathematical description of the diagenetic behavior of a large number of dissolved and solid-sediment species that are related through interconversion reactions and/or by their production or consumption during organic-matter decay. A well formulated pH model is perhaps the ultimate test of our understanding of the anoxic porewater system because it attempts to fit together all the often separately acquired bits of this geochemical puzzle.

The work in this paper represents only a first step in this direction. That we were obliged to introduce some *ad hoc* free parameters in order to solve the model for our chosen example is in no way a failure of the approach, but simply a reflection of our

imperfect knowledge of this complex system and the lack of a suitably broad data base.

Acknowledgments. We thank M. Goldhaber and J. Mackin for their insightful reviews. B. P. Boudreau received financial support from NSERC Grant #U0506, and D. Canfield was supported by NSF Grants OCE 8219580 and 8508472 (R. Berner, Yale University, P.I.).

APPENDIX

The coupled system of differential-algebraic equations that form the model are solved by a semianalytic iterative technique. As a first step, the unknown R-terms for fast acid-base interconversions, i.e. R_{C1}, R_{C2}, R_S, R_N, R_{P1}, R_{P2}, R_{P3}, and R_B, and the FeS precipitation reaction, R_{FeS}, are eliminated by manipulating Eqs. (1) through (17). Without dwelling on the details of these algebraic manipulations (see Boudreau (1987) or Olander (1960) for informative examples), the resulting reduced set of *linear* ODEs is

$$\begin{aligned} &D_H[H]'' - D_{OH}[OH]'' + 2D_{H_2S}[H_2S]'' + D_{HS}[HS]'' + 2D_{CO_2}[CO_2]'' \\ &\quad + D_{HCO_3}[HCO_3]'' + D_{NH_4}(NH_4]'' - D_{H_2PO_4}[H_2PO_4]'' - 2D_{HPO_4}[HPO_4]'' \\ &\quad - 3D_{PO_4}[PO_4]'' + D_{B(OH)_3}[B(OH)_3]'' + \left[2 - \left(\frac{f+g}{2}\right)\right]\Sigma\alpha_i e^{-\beta_i x} \\ &\quad = v[[H]' - [OH]' + 2[H_2S]' + [HS]' + 2[CO_2]' + [HCO_3]' \\ &\quad + (1 + K_{ads}^N)[NH_4]' - (1 + K_{ads}^P)\{[H_2PO_4]' + 2[HPO_4]' \\ &\quad + 3[PO_4]'\} + [B(OH)_3]'] \end{aligned} \tag{A1}$$

$$D_{H_2S}[H_2S]'' + D_{HS}[HS]'' - D_{Fe}[Fe]'' + \tfrac{1}{2}(1 - g - h)\Sigma\alpha_i e^{-\beta_i x} = v[[H_2S]' + [HS]' - [Fe]'] \tag{A2}$$

$$D_{CO_2}[CO_2]'' + D_{HCO_3}[HCO_3]'' + D_{CO_3}[CO_3]'' + \Sigma\alpha_i e^{-\beta_i x} - \kappa e^{-\epsilon x} = v[[CO_2]' + [HCO_3]' + [CO_3]'] \tag{A3}$$

$$D_{NH_3}[NH_3]'' + D_{NH_4}[NH_4]'' + y\Sigma\alpha_i e^{-\beta_i x} = v[[NH_3]' + (1 + K_{ads}^N)[NH_4]'] \tag{A4}$$

$$\begin{aligned} &D_{H_3PO_4}[H_3PO_4]'' + D_{H_2PO_4}[H_2PO_4]'' + D_{HPO_4}[HPO_4]'' + D_{PO_4}[PO_4]'' \\ &\quad + z\Sigma\alpha_i e^{-\beta_i x} = v[[H_3PO_4]' + (1 + K_{ads}^P)\{[H_2PO_4]' + [HPO_4]' \\ &\quad + [PO_4]'\}] \end{aligned} \tag{A5}$$

$$D_{B(OH)_3}[B(OH)_3]'' + D_{B(OH)_4}[B(OH)_4]'' = v[[B(OH)_3]' + [B(OH)_4]'] \tag{A6}$$

$$D_{Ca}[Ca]'' - v[Ca]' - \kappa e^{-\epsilon x} = 0 \tag{A7}$$

With Eqs. (18) through (27), this system of 17 differential-algebraic equations governs the distributions of the 17 unknown concentrations with depth.

As written, this system of equations appears to have no simple analytical solution.

However, if the advection terms (i.e. the first derivatives on the right-hand side of Eqs. (A1) to (A6)) were not present, then Boudreau (1987) has shown that an implicit analytical solution is possible. These advection terms are unlikely to be the dominant transport terms of these mass balances. As a reasonable initial estimate of the correct solution, one could assume these terms to be zero (Lin and Segel, 1974, p. 238–240).

The resulting linear ODEs as well as Eq. (A7) can be integrated twice (e.g. see the Appendix in Boudreau, 1987) to obtain seven more algebraic equations. Combined with the ten other nonlinear thermodynamic relationships, i.e. Eqs. (18) through (27), the solution to these implicit equations provides an initial estimate for the concentration profiles.

With this initial solution in hand, Eqs (A1) through (A6) can be reconsidered. If we substitute our initial solution into the right-hand side of each of these equations, then the advective terms act as known correction terms. The linear system of ODEs can be solved again with these known corrections and combined with the thermodynamic constraints to produce the first iterated solution (i.e. profiles). This process is repeated until the iterated solutions converge to within a proscribed error.

Examination of the equations generated by this technique reveals that the equations for each iteration have the same form. Thus, for the n-th iteration ($n = 0, 1, 2, \ldots$), the concentrations must satisfy the following equations in addition to the Eqs. (18) through (27),

$$[B(OH)_3]_n = \frac{a_6 + v[I_{B(OH)_3} + I_{B(OH)_4}]}{\left[D_{B(OH)_3} + \dfrac{D_{B(OH)_4}K_B}{[H]_n}\right]} \tag{A8}$$

$[HPO_4]_n$

$$= \frac{a_5 + v(1 + K^P_{ads})[I_{H_2PO_4} + I_{HPO_4} + I_{PO_4}] + z\sum \dfrac{\alpha_i}{\beta_i^2}(1 - e^{-\beta_i x}) - \dfrac{\alpha_i x}{\beta_i} e^{-\beta_i L}}{\left[\dfrac{D_{H_2PO_4}[H]_n}{K_{P2}} + D_{HPO_4} + \dfrac{D_{PO_4}K_{P3}}{[H]_n}\right]} \tag{A9}$$

$$[NH_4]_n = \frac{a_4 + v(1 + K^N_{ads})[I_{NH_3} + I_{NH_4}] + y\sum \dfrac{\alpha_i}{\beta_i^2}(1 - e^{-\beta_i x} - \dfrac{\alpha_i x}{\beta_i} e^{-\beta_i L}}{\left[\dfrac{D_{NH_3}}{K_N[H]_n} + D_{NH_4}\right]} \tag{A10}$$

$$[HCO_3]_n = \frac{F(x)}{\left[\dfrac{D_{CO_2}[H]_n}{K_{C1}} + D_{HCO_3} + \dfrac{D_{CO_3}K_{C2}}{[H]_n}\right]} \tag{A11}$$

$$[HS]_n = \frac{-B_n + (B_n^2 - 4A_nC_n)^{1/2}}{2A_n} \tag{A12}$$

$$D_H[H]_n - D_{OH}[OH]_n + 2D_{H_2S}[H_2S]_n + D_{HS}[HS]_n + 2D_{CO_2}[CO_2]_n + D_{HCO_3}[HCO_3]_n + D_{NH_4}[NH_4]_n - D_{H_2PO_4}[H_2PO_4]_n - 2D_{HPO_4}[HPO_4]_n - 3D_{PO_4}[PO_4]_n + D_{B(OH)_3}[B(OH)_3]_n + \left[2 - \left(\frac{f+g}{2}\right)\right]\left[\sum \frac{\alpha_i}{\beta_i^2}(1 - e^{-\beta_i x}) - \sum \frac{\alpha_i x}{\beta_i} e^{-\beta_i L}\right] = a_1 + v[I_H - I_{OH} + 2I_{H_2S} + I_{HS} + 2I_{CO_2} + I_{HCO_3} + (1 + K^N_{ads})I_{NH_4} - (1 + K^P_{ads})(I_{H2PO_4} + 2I_{HPO_4} + 3I_{PO_4}) + I_{B(OH)_3}] \quad (A13)$$

where

$$F(x) \equiv a_3 + [I_{CO_2} + I_{HCO_3} + I_{CO_3}] - \frac{\kappa}{\epsilon^2}(1 - e^{-\kappa x}) + \frac{\kappa x}{\epsilon} e^{-\epsilon L} + \sum \left[\frac{\alpha_i}{\beta_i^2}(1 - e^{-\beta_i x}) - \frac{\alpha_i x}{\beta_i} e^{-\beta_i L}\right] \quad (A14)$$

$$A_n \equiv \frac{D_{H_2S}[H]_n}{K_S} + D_{HS} \qquad C_n \equiv -\frac{D_{Fe}[H]_n}{K_{FeS}} \quad (A15, A16)$$

$$B_n \equiv -\left[a_2 + v(I_{H_2S} + I_{HS} - I_{Fe}) + \frac{(1 - g - h)}{2} \sum \left[\frac{\alpha_i}{\beta_i^2}(1 - e^{-\beta_i x}) - \frac{\alpha_i x}{\beta_i} e^{-\beta_i L}\right]\right] \quad (A17)$$

$$a_1 \equiv D_H H(0) - D_{OH}OH(0) + 2D_{H_2S}H_2S(0) + D_{HS}HS(0) + 2D_{CO_2}CO_2(0) + D_{HCO_3}HCO_3(0) + D_{NH_4}NH_4(0) - D_{H_2PO_4}H_2PO_4(0) - 2D_{HPO_4}HPO_4(0) - 3D_{PO_4}PO_4(0) + D_{B(OH)_3}B(OH)_3(0) \quad (A18)$$

$$a_2 \equiv D_{H_2S}H_2S(0) + D_{HS}HS(0) - D_{Fe}Fe(0) \quad (A19)$$

$$a_3 \equiv D_{CO_2}CO_2(0) + D_{HCO_3}HCO_3(0) + D_{CO_3}CO_3(0) \quad (A20)$$

$$a_4 \equiv D_{NH_3}NH_3(0) + D_{NH_4}NH_4(0) \quad (A21)$$

$$a_5 \equiv D_{H_3PO_4}H_3PO_4(0) + D_{H_2PO_4}H_2PO_4(0) + D_{HPO_4}HPO_4(0) + D_{PO_4}PO_4(0) \quad (A22)$$

$$a_6 \equiv D_{B(OH)_3}B(OH)_3(0) + D_{B(OH)_4}B(OH)_4(0) \quad (A23)$$

$$I_i \equiv \int_0^x [C_i]_{n-1} - [C_i]_{n-1}(L)dx \quad (A24)$$

and where $[C_i]_n$ is the concentration of the i-th species at depth x on the n-th iteration, and $[C_i]_{n-1}(L)$ is the concentration of the i-th species at depth L (base of the model) on the $(n-1)$ iteration. If $n = 0$, then $I_i \equiv 0$. The implicit nature of the solution means that Eq. (A23) must be evaluated numerically.

Because $[H_3PO_4] \ll [H_2PO_4]$, $[HPO_4]$ and $[PO_4]$, all terms involving $[H_3PO_4]$ have been dropped from Eq. (A9) for simplicity.

To summarize the solution method: (1) evaluate with the data from the previous iteration Eq. (A24) if $n \neq 0$; (2) guess a value of $[H]_n$ at a depth, x, of interest; (3) Solve Eqs. (A8) through (A12) and then Eqs. (18) through (26) to obtain the concentrations of the dissolved species that correspond to this guessed value of $[H]_n$; (4) check the correctness of $[H]_n$ by solving Eq. (A13); (5) guess a new value of $[H]_n$ (by bisection) until Eq. (A13) is satisfied; repeat this process for the next depth of interest and, in this manner, create the profiles that correspond to the n-th iterate; (6) compare the profiles with the last iterate. If they agree to within a nominal error, then stop; these are the acceptable profiles. If they disagree beyond the stated error, then start the calculations again at step (1) using this past iteration in Eq. (A24).

REFERENCES

Aller, R. C. 1980a. Diagenetic processes near the sediment-water interface of Long Island Sound. I. Decomposition and nutrient element geochemistry (S,N,P). Adv. Geophys., *22*, 237–350.

—— 1980b. Diagenetic processes near the sediment-water interface of Long Island Sound. II. Fe and Mn. Adv. Geophys., *22*, 351–415.

—— 1982. Carbonate dissolution in nearshore terrigenous muds: the role of physical and biological reworking. J. Geol., *90*, 79–95.

Aller, R. C. and P. D. Rude. 1986. Anoxic oxidation of sulfides in marine sediments. EOS, *67*, 996.

Anderson, D. E. 1981. Diffusion in electrolyte mixtures, *in* Kinetics of Geochemical Processes, A. C. Lasaga and R. J. Kirkpatrick, eds., Mineral. Soc. America, 398 pp.

Ben-Yaakov, S. 1972. Diffusion of sea water ions.-I. Diffusion of sea water into a dilute solution. Geochim. Cosmochim. Acta, *36*, 1397–1406.

—— 1973. pH buffering of pore water of recent anoxic marine sediments. Limnol. Oceanogr., *18*, 86–94.

—— 1981. Diffusion of seawater ions: significance and consequences of cross coupling effects. Am. J. Sci., *281*, 974–980.

Berner, R. A. 1967. Thermodynamic stability of sedimentary iron sulfides. Am. J. Sci., *265*, 773–785.

—— 1969. Chemical changes affecting dissolved calcium during the bacterial decomposition of fish and clams in sea water. Mar. Geol., *7*, 253–274.

—— 1970. Sedimentary pyrite formation. Am. J. Sci., *268*, 1–23.

—— 1975. The role of magnesium in the crystal growth of calcite and aragonite from sea water. Geochim. Cosmochim. Acta, *39*, 489–504.

—— 1977. Stoichiometric models for nutrient regeneration in anoxic sediments. Limnol. Oceanogr., *22*, 781–786.

—— 1980. Early Diagenesis: A Mathematical Approach. Princeton University Press, Princeton, NJ, 241 pp.

—— 1981. A new geochemical classification of sedimentary environments. J. Sed. Petrol., *51*, 359–365.

—— 1984. Sedimentary pyrite formation: an update. Geochim. Cosmochim. Acta, *48*, 605–615.

Berner, R. A., M. R. Scott and C. Thomlinson. 1970. Carbonate alkalinity in the pore waters of anoxic marine sediments. Limnol. Oceanogr., *15,* 544–549.

Berner, R. A. and J. T. Westrich. 1985. Bioturbation and early diagenesis of carbon and sulfur. Am. J. Sci., *285,* 193–206.

Berner, R. A., J. T. Westrich, R. Graber, J. Smith and C. S. Martens. 1978. Inhibition of aragonite precipitation from supersaturated seawater: a laboratory and field study. Am. J. Sci., *278,* 816–837.

Boudreau, B. P. 1987. A steady-state diagenetic model for dissolved carbonate species and pH in the porewaters of oxic and suboxic sediments. Geochim. Cosmochim. Acta, *51,* 1985–1996.

Boudreau, B. P. and J. T. Westrich. 1984. The dependence of bacterial sulfate reduction on sulfate concentration in marine sediments. Geochim. Cosmochim. Acta, *48,* 2503–2516.

Boulegue, J., C. J. Lord and T. M. Church. 1982. Sulfur speciation and associated trace metals (Fe,Cu) in the pore waters of Great Marsh, Delaware. Geochim. Cosmochim. Acta, *46,* 453–464.

Canfield, D. E. 1988. Sulfate reduction and the diagenesis of iron in anoxic marine sediments. Ph.D. thesis, Yale University, New Haven, CT, 248 pp.

Canfield, D. E. and R. A. Berner. 1987. Dissolution and pyritization of magnetite in anoxic marine sediments. Geochim. Cosmochim. Acta, *51,* 645–659.

Chang, C.-S. and G. T. Rochelle. 1982. Mass transfer enhanced by equilibrium reactions. Indus. Eng. Chem. Fund., *21,* 379–385.

Danckwerts, P. V. 1970. Gas-Liquid Reactions, McGraw-Hill, NY, 276 pp.

Devol, A. H., J. J. Anderson, K. Kuivila and J. W. Murray. 1984. A model for the coupled sulfate reduction and methane oxidation in the sediments of Saanich Inlet. Geochim. Cosmochim. Acta, *48,* 993–1004.

DiToro, D. M. 1976. Combining chemical equilibrium and phytoplankton models—A general methodology, *in* Modeling Biochemical Processes in Aquatic Ecosystems, R. P. Canale, ed., Ann Arbor Science, 389 pp.

Drever, J. I. 1971. Magnesium-iron replacement in clay minerals in anoxic sediments. Science, *172,* 1334–1336.

Emerson, S., L. Jacobs and B. Tebo. 1983. The behavior of trace metals in marine anoxic waters: solubilities at the oxygen-hydrogen sulfide interface, *in* Trace Metals in Sea Water, C. S. Wong, E. Boyle, K. W. Bruland, J. D. Burton and E. D. Goldberg, eds., Plenum Press, NY, 920 pp.

Francois, R. 1987. A study of sulfur enrichment in the humic fraction of marine sediments during early diagenesis. Geochim. Cosmochim. Acta, *51,* 17–27.

Gallagher, P. M., A. L. Athayde and C. F. Ivory. 1986. The combined flux technique for diffusion-reaction problems in partial equilibrium: application to facilitated transport of carbon dioxide in aqueous bicarbonate solutions. Chem. Eng. Sci., *41,* 567–578.

Gardner, L. R 1973. Chemical models for sulfate reduction in closed anaerobic marine environments. Geochim. Cosmochim. Acta, *37,* 53–68.

Goldhaber, M. B., R. C. Aller, J. K. Cochran, J. K. Rosenfeld, C. S. Martens and R. A. Berner. 1977. Sulfate reduction, diffusion, and bioturbation in Long Island Sound sediments: report of the FOAM Group. Am. J. Sci., *277,* 193–237.

Goldhaber, M. B. and I. R. Kaplan. 1974. The sulfur cycle, *in* The Sea, Marine Chemistry, E. D. Goldberg, ed., v. 5, John Wiley & Sons, NY, 895 pp.

—— 1975. Apparent dissociation constants of hydrogen sulfide in chloride solutions. Mar. Chem., *3,* 83–104.

Heller-Kallai, L. and I. Rozenson. 1978. Removal of magnesium from interstitial waters in

reducing environments—the problem reconsidered. Geochim. Cosmochim. Acta, *42*, 1907–1909.

Horne, R. A. 1969. Marine Chemistry. Wiley-Interscience, NY, 568 pp.

Iversen, N. and B. B. Jorgensen. 1985. Anaerobic methane oxidation rates at the sulfate-methane transition in marine sediments from Kattegat and Skagerrak (Denmark). Limnol. Oceanogr., *30*, 944–955.

Johnson, K. S. 1982. Carbon dioxide hydration and dehydration kinetics in seawater. Limnol. Oceanogr., *27*, 849–855.

Katz, A. and S. Ben-Yaakov. 1980. Diffusion of seawater ions. Part II. The role of activity coefficients and ion pairing. Mar. Chem., *8*, 263–280.

Kester, D. R. and R. M. Pytkowicz. 1967. Determination of the apparent dissociation constants of phosphoric acid in seawater. Limnol. Oceanogr., *12*, 243–252.

Krishnaswami, S., M. C. Monaghan, J. T. Westrich, J. T. Bennett and K. K. Turekian. 1984. Chronologies of sedimentary processes in sediments of the FOAM Site, Long Island Sound, Connecticut. Am. J. Sci., *284*, 706–733.

Krom, M. D. and R. A. Berner. 1980. The diffusion coefficients of sulfate, ammonium and phosphate ions in anoxic marine sediments. Limnol. Oceanogr., *25*, 327–337.

—— 1981. The diagenesis of phosphorus in a nearshore marine sediment. Geochim. Cosmochim. Acta, *45*, 207–216.

Lasaga, A. C. 1979. The treatment of multi-component diffusion and ion pairs in diagenetic fluxes. Am. J. Sci., *279*, 324–346.

—— 1981a. Influence of diffusion coupling on diagenetic concentration profiles. Am. J. Sci., *281*, 553–575.

—— 1981b. The treatment of multi-component diffusion and ion pairs in diagenetic fluxes: further comments and clarification. Am. J. Sci., *281*, 981–988.

Li, Y.-H. and S. Gregory. 1974. Diffusion of ions in sea water and in deep-sea sediments. Geochim. Cosmochim. Acta, *38*, 703–714.

Lin, C. C. and L. A. Segel. 1974. Mathematics Applied to Deterministic Problems in the Natural Sciences. Macmillan, NY, 604 pp.

Lyman, J. 1956. Buffer mechanism of seawater. Ph.D. thesis, Univ. California, Los Angeles, CA, 196 pp.

Mackenzie, F. T. and R. M. Garrels. 1966. Chemical mass balance between rivers and oceans. Am. J. Sci., *264*, 507–525.

Mackin, J. E. 1986a. The free-solution diffusion coefficient of boron: influence of dissolved organic matter. Mar. Chem., *20*, 131–140.

—— 1986b. Control of dissolved Al distributions in marine sediments by clay reconstitution reactions: Experimental evidence leading to a unified theory. Geochim. Cosmochim. Acta, *50*, 207–217.

—— 1987. Boron and silica behavior in salt-marsh sediments: implications for paleo-boron distributions and the early diagenesis of silica. Am. J. Sci., *287*, 197–241.

Mackin, J. E. and R. C. Aller. 1984. Dissolved Al in sediments and waters of the East China Sea: Implications for authigenic mineral formation. Geochim. Cosmochim. Acta, *48*, 281–297.

Mackin, J. E. and K. T. Swider. 1987. Modeling the dissolution behavior of standard clays in seawater. Geochim. Cosmochim. Acta, *51*, 2947–2964.

Martens, C. S., R. A. Berner and J. K. Rosenfeld. 1978. Interstitial water chemistry of anoxic Long Island Sound sediment. 2. Nutrient regeneration and phosphate removal. Limnol Oceanogr., *23*, 605–617.

Martens, C. S. and J. V. Klump. 1984. Biogeochemical cycling in an organic-rich coastal marine

basin. 4. An organic carbon budget for sediments dominated by sulfate reduction and methanogenesis. Geochim. Cosmochim. Acta, *48,* 1987–2004.

Mehrbach, C., C. H. Culbersen, J. E. Hawley and R. M. Pytkowicz. 1973. Measurement of the apparent dissociation constants of carbonic acid in seawater at atmospheric pressure. Limnol. Oceanogr., *18,* 897–907.

Millero, F. J. 1983. The estimation of the pK^*_{HA} of acids in seawater using the Pitzer equations. Geochim. Cosmochim. Acta, *47,* 2121–2129.

Millero, F. J. and D. R. Schreiber. 1982. Use of the ion pairing model to estimate activity coefficients of the ionic components of natural waters. Am. J. Sci., *282,*1508–1540.

Morel, F. M. M. 1983. Principles of Aquatic Chemistry. John Wiley and Sons, NY, 446 pp.

Murray, J. W., V. Grundmanis and W. M. Smethie. 1978. Interstitial water chemistry in the sediments of Saanich Inlet. Geochim. Cosmochim. Acta, *42,* 1011–1026

Nissenbaum, A., B. J. Presley and I. R. Kaplan. 1972. Early diagenesis in a reducing fjord, Saanich Inlet, British Columbia—I. Chemical and isotopic changes in major components of interstitial water. Geochim. Cosmochim. Acta, *36,* 1007–1027.

Olander, D. R. 1960. Simultaneous mass transfer and equilibrium chemical reaction. Am. Inst. Chem. Eng. J., *6,* 233–239.

Otto, N. C. and J. A. Quinn. 1971. The facilitated transport of carbon dioxide through bicarbonate solutions. Chem. Eng. Sci., *26,* 949–961.

Pytkowicz, R. M. 1983. Equilibria, Nonequilibria, and Natural Waters, II. Wiley-Interscience, NY, 353 pp.

Pyzik, A. J. and S. E. Sommer. 1981. Sedimentary iron monosulfides: kinetics and mechanism of formation. Geochim. Cosmochim. Acta, *45,* 687–698.

Redfield, A. C., B. H. Ketchum and F. A. Richards. 1963. The influence of organisms on the composition of seawater, *in* The Sea, M. N. Hill, ed., v. 2, Wiley-Interscience, NY, 554 pp.

Reeburgh, W. S. 1976. Methane consumption in Cariaco Trench waters and sediment. Earth Planet. Sci. Lett., *28,* 337–344.

—— 1980. Anaerobic methane oxidation: rate depth distribution in Skan Bay sediments. Earth Planet. Sci. Lett., *47,* 345–352.

Rickard, D. T. 1974. Kinetics and mechanism of sulfidation of goethite. Am. J. Sci., *274,* 941–952.

—— 1975. Kinetics and mechanism of pyrite formation at low temperatures. Am. J. Sci., *275,* 636–652.

Rosenfeld, J. K. 1977. Nitrogen diagenesis in nearshore anoxic sediments. Ph.D. thesis, Yale Univ., New Haven, CT, 191 pp.

—— 1981. Nitrogen diagenesis in Long Island Sound sediments. Am. J. Sci., *281,* 436–462.

Rubin, J. 1983. Transport of reacting solutes in porous media: relation between mathematical nature of problem formulation and chemical nature of reactions. Water Resources Res., *19,* 1231–1252.

Rudd, J. W. M., C. A. Kelly and A. Furutani. 1986. The role of sulfate reduction in the long term accumulation of organic and inorganic sulfur in lake sediments. Limnol. Oceanogr., *31,* 1281–1291.

Shampine, L. F. and C. W. Gear. 1979. A user's view of solving stiff ordinary differential equations. Soc. Indus. Appl. Math. Rev., *21,* 1–17.

Sherwood, T. K., R. L. Pigford and C. R. Wilke. 1975. Mass Transfer. McGraw-Hill, NY, 677 pp.

Sholkovitz, E. 1973. Interstitial water chemistry of the Santa Barbara Basin sediments. Geochim. Cosmochim. Acta, *37,* 2043–2073.

Thorstenson, D. C. 1970. Equilibrium distribution of small organic molecules in natural waters. Geochim. Cosmochim. Acta, *34*, 745–770.

Westrich, J. T. 1983. The consequences and controls of bacterial sulfate reduction in marine sediments. Ph.D. thesis, Yale Univ., New Haven, CT, 530 pp.

Received: *20 July 1987;* revised: *16 December, 1987.*